ENCASED CANTILEVERS FOR LOW-NOISE FORCE AND MASS SENSING IN LIQUIDS

D. Ziegler[1], A. Klaassen[2], D. Bahri[1], D. Chmielewski[1], A. Nievergelt[1], F. Mugele[2], J.E. Sader[3], and P.D. Ashby[1]*

[1]Lawrence Berkeley National Laboratory, Berkeley, USA

[2] University of Twente, Twente, THE NETHERLANDS

[3] University of Melbourne, Melbourne, AUSTRALIA

ABSTRACT

Viscous damping severely limits the performance of resonator based sensing in liquids. We present encased cantilevers that overcome this limitation with a transparent and hydrophobic encasement built around the resonator. Only a few micrometers of the cantilever probe protrude from the encasement and water does not enter the encasement. This maintains high Q-factors and reduces the thermo-mechanical noise levels by over one order of magnitude and reaches minimal detectable forces of 12 fN/•Hz in liquids. These probes expand the frontiers of cantilever based sensing. We discuss their design and fabrication with special focus on squeeze film damping and demonstrate their successful application for quantitative mass sensing of single nanoparticles and gentle Atomic Force Microscopy imaging of soft matter in liquids.

INTRODUCTION

One of the most prominent applications of mechanical resonators is Atomic Force Microscopy (AFM)[1], which takes a topographic image by scanning a sharp tip attached to a cantilever over a surface while measuring the interaction forces through the change in the cantilever's deflection, resonance frequency, or oscillation amplitude. Beyond height information it enables visualization of materials properties such as magnetism[2], specific chemical interactions[3], [4], or electrical properties at high resolution [5]. Its resolution, label-free detection, and extended observation time without damage or bleaching, lift AFM to arguably the best tool to study the structure and behavior of biomolecules at surfaces[6], [7], [8]. Another application of mechanical resonators, which emerged in the mid-1990s, is chemical or bio-sensing[9] and is today a well-known technique for cheap, portable, analysis systems [10],[11]. The minimum detectable forces or mass changes are associated with losses due to damping of the resonator arising from the exchange of energy between the resonator and its surrounding environment [12], [13]. The smallest measurable force is given by $F_n=(2kk_bTB/\pi Qf_0)^{\wedge}1/2$, where k is the spring constant, k_bT is the thermal energy, B the measurement bandwidth, Q the mechanical quality factor, and f_0 the resonance frequency. Upon immersion in water, a typical cantilever's resonance frequency drops about by a factor of three and its Q-factor by a factor of 50. Compared to operation in air, the resulting smallest detectable force is increased by more than one order of magnitude.

Researchers have been attempting to decrease viscous damping by reducing the size of the cantilever[14], [15] or keep the resonator in air such that only the sensing tip is immersed in solution. Practically, the latter has been difficult to achieve. The few attempts so far include bell jar designs for length extensional resonators[16], tuning forks[17], or optical fiber probes[18]. But in all these designs the resonator and their enclosures are so large, that their size offsets gains due to lower viscosity, furthermore, they all demand specialized instrumentation and cannot be used with standard AFM instruments. Here, we present a solution, where a transparent encasement is directly fabricated around the cantilever with only the tip protruding from the encasement (see Figure 1a). As the encasement is transparent these probes can be used on any commercially available AFM without modification of the instrument.

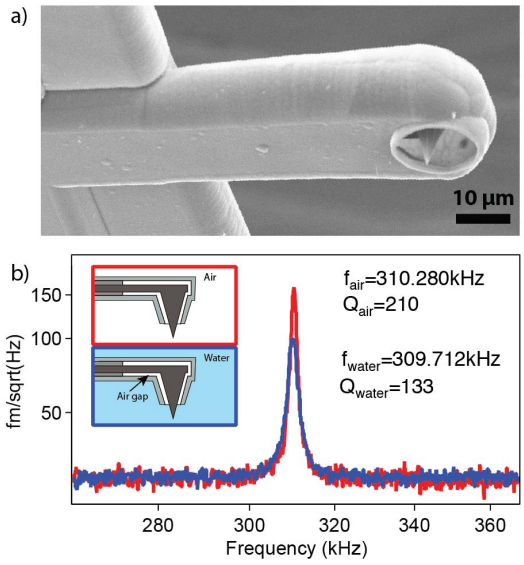

Figure 1: a) Electron microscope image of an encased cantilever b) Thermal noise spectra recorded in air (red curve) and water (blue curve) show that exceptionally high Q-factor and resonance frequency are mainainted while operating in liquids. Note that without the encasement immersion in water would lower the resonance frequency by about a factor three and the Q-factor would drop by a factor of 50.

Once immersed in liquid, the hydrophobic interior of the encasement pins the air-water interface at the orifice preventing water from entering, and the cantilever effectively vibrates in air. The thermal spectra shown in figure 1b) clearly reveal that a high resonance frequency and Q factor are maintained while submerged in water. The resulting smallest detectable force in liquid of 12 fN/√Hz

outperforms regular non-encased cantilevers (150 fN/√Hz) by more than one order of magnitude.

FABRICATION

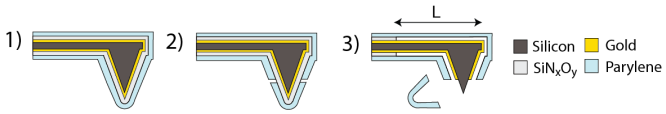

Figure 2: Simplified illustration of the mask-less process to fabricate encased cantilevers. 1) Deposition of a thick sacrificial silicon oxynitride (gap) and Parylene layer (encasement) on commercially available gold-coated silicon cantilevers. 2) Focused ion beam opening of the Parylene layer around the apex. 3) A hydrofluoric acid wet etch releases the cantilever and defines its final length (L).

A simplified fabrication process of the encasement is illustrated in figure 2. In the first step (1) regular gold coated silicon cantilevers with a nominal width of 35 µm, thickness of 1 µm, and a length of 90,110, and 130 µm (NSC36, Mikromasch) are coated with a sacrificial layer of silicon oxynitride using plasma enhanced chemical vapor deposition (PECVD, Plasmalab80 Plus, Oxford Instruments). Deposition using 1182 sccm of 1%SiH_4/Ar and 710 sccm of N_2O, at 350ºC and a pressure of 1000 mbar results in a rate of about 140 nm/min. The resulting low stress oxynitride layer reduces bending of the cantilever and its low quality gives conveniently high etch rates in the subsequent release process. The encasement itself consists of a uniformly deposited 2 µm thick poly(p-xylylene) layer (Parylene C, PDS2010, SCS). In the next step (2) we use focused ion beam milling (FIB, 1540ESB, Zeiss) to cut a roughly 0.5 µm wide opening around the cantilever's tip. This exposes the sacrificial layer and enables releasing of the cantilever by a hydrofluoric acid etch (>40% HF) (3). Note that the length of the final cantilever (L) is adjusted by the time of this etch step. The cap falls off during etching and the tip apex protrudes from the encasement. The protecting gold layer can be selectively removed from the apex only (wet gold etch, G1814, Transene). Transmission electron microscopy (TEM) and using AFM confirmed that the fabrication process does not affect probe sharpness and a radius smaller than 10 nm is preserved.

SQUEEZE FILM DAMPING

The thickness of the sacrificial layer is an important design parameter because it defines the gap size, which determines how much the tip protrudes. But the gap size also influences squeeze film damping as discussed in this section. Figure 3 a) shows a cross-section of an encased cantilever, where the red arrows indicate the flow of air inside the encasement when the cantilever moves upwards. The built-up pressure inside the encasement leads to a special type of viscous damping in confined spaces known as squeeze film damping (SFD). This phenomenon has been studied to optimize MEMS resonators[19], [20], but these designs commonly experience SFD on only one side of the resonator. In encased cantilevers, however, the effect is two-sided and thus it is unknown for which gap size SFD starts deteriorating the device's performance. Modeling squeezed films involves coupling the modified Reynolds equation with the equations for the structural displacements which remains a challenging mathematical problem until today[21]. Hence, we used finite elements to model the hydrostatic pressures and fluid/solid interactions inside the encasement (FLUID80 model, ANSYS).

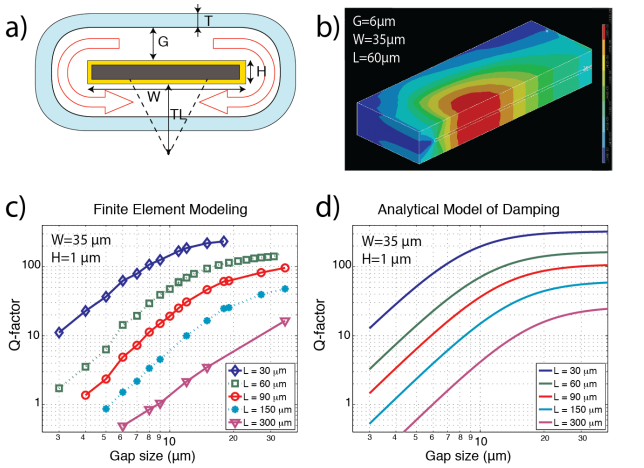

Figure 3: Squeeze film damping in encased cantilevers a) Cross-section of an encased cantilever (not to scale) the gap size (G), encasement thickness (T), cantilever thickness (H), width (W) and tip length (TL) are indicated. b) Pressure distribution inside cavity c) Q-factors for different gap size (G) and cantilever length (L) extracted by FEM simulations. d) Analytical models of squeeze film damping using Sader equations.

Figure 3b) shows a longitudinal cross-section of the air volume inside the gap. The color scale shows the absolute value of the pressure upon motion of the cantilever. The pressure is highest near the free end of the cantilever where displacement is greatest. The high pressure extends to the encasement surface pushing the air around the side of the cantilever and increasing damping. By fitting a simple harmonic oscillator model to the power spectrum of the calculated cantilever thermal motion, we extract resonance frequency and damping of the cantilever. Figure 3c) shows the Q-factor as a function of gap size for five different cantilever lengths (L) computed using this finite element model.

The damping cantilevers can be calculated analytically in the extreme cases of being completely dominated by squeeze film damping (G<<W/2) [22],[23] and when completely unbounded (G>>W) [13]. For encased cantilever we assume a doubling in the squeeze film damping and we approximate the transition between the two extremes with the function A/(1+B/(G/W)^3) where A is the unbounded Q factor and B is the coefficient matching the behavior of the doubly bounded system at small gap (see figure 3d). Our findings from the finite element analysis and hydrodynamic models are in good qualitative agreement and clearly show

that SFD only becomes significant for G<<W/2. For most commercially available cantilevers this is difficult to achieve, because as illustrated in Figure 3a), the tip length (TL) is required to be larger than G+T for the tip to protrude into the liquid (see Figure 3a).

APPLICATIONS

Gentle Imaging of Soft Matter

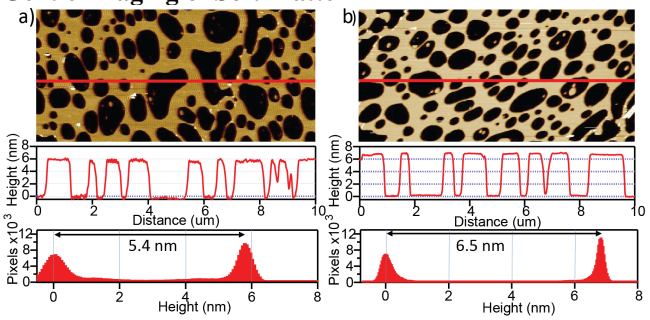

Figure 4: DPPC lipid bilayers supported on mica measured using regular silicon nitride cantilevers (a)) and encased cantilevers (b)). The cross-sections and histogram analysis clearly reveals a higher measured thickness of the bilayer when measured with encased cantilevers, which demonstrates that soft samples deform less.

High viscous damping has limited the AFM's utility for imaging soft materials in solution at high resolution without deforming or even damaging the samples[25]. As lipid bilayers readily deform under the force applied by the tip, it is a useful sample to demonstrate the gentleness of encased cantilevers. Supported DPPC lipid bilayers (L-α-dipalmitoyl-phosphatidylcholine) are prepared using a Langmuir-Blodgett trough, transferred onto mica and imaged in aqueous buffer. While the softest possible imaging with conventional silicon nitride cantilevers (Hydra Cantilevers, Applied Nanosciences Inc., Santa Clara CA, USA) results in a height of 5.4 nm (figure 2a) we obtain a thickness of 6.5 nm when using encased cantilevers (figure 2b). This exceeds the highest previously reported thickness using AFM [26], and clearly demonstrates gentle imaging enabled by the low damping.

Quantitative Mass Sensing

Cantilever based mass sensors detect minute amounts of specific chemicals or biomolecules and may significantly impact biological and chemical diagnostics. The resonance frequency shift of a cantilever is a direct measure of the added mass, but the challenge of measuring resonance frequency in a high damping/low Q-factor environment leads many sensor incarnations to indirectly measure adsorbed material using static deflection caused by surface stress[27]. The low damping of encased cantilevers, however, enables in-situ mass sensing in liquids that surpasses conventional cantilever based mass sensing, where the uncertainty of the location of the added mass, or the indirect measurement of stress induced bending require various assumptions or models in order to extract the exact value of the added mass [28],[29]. For encased cantilevers, functionalization and binding of an analyte only occur at the tip (figure 5a). Compared to a uniform loading, this confined location of the added mass results in better responsivity, R_p, Responsivity takes into account a normalizing effective mass ($m^*=n_e\ m_c$, with $n_e \approx 0.24$) (see Eq.1).

$$R_p = \frac{\Delta f}{\Delta m} = -2\pi^2 \frac{f_0^3}{k_c} = -\frac{1}{2n_e}\frac{f_0}{m_c}. \qquad (1)$$

As the mass of the cantilever (m_c) is known, the added mass (Δm) can be extracted quantitatively from the measured frequency shift (Δf) [30]. Combined with a factor 20 of improvement from maintaining high resonance frequency f_0 and Q-factor a 80-fold reduction of the smallest detectable mass (δm) is achieved compared to a non-encased cantilever.

$$\delta m = -\frac{1}{\pi A_c}\sqrt{\frac{2k_B T B n_e m_c}{f_0^3 Q}}. \qquad (2)$$

where A_c is the oscillation amplitude. The concept of quantitative mass sensing is confirmed by measuring the mass of gold particles.

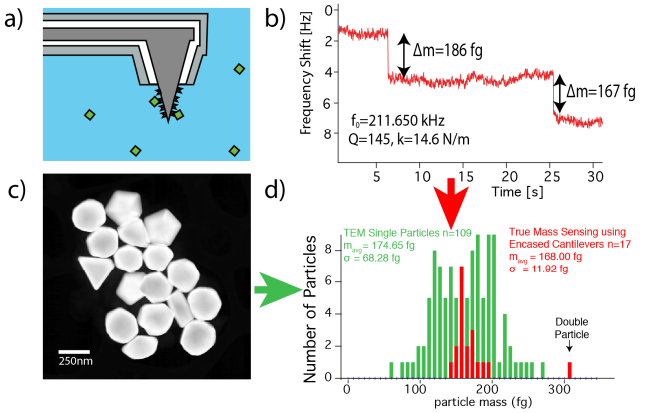

Figure 5: Encased cantilevers for mass sensing in liquids, a) local functionalization and attachment of the analyte at the tip b) the frequency shifts upon attachment of 250 nm gold particles and a corresponding added average mass of 169 fg was found c) TEM image of the gold particles, d) histogram of the estimated mass using TEM (green) and encased cantilevers as mass sensors (red).

Figure 5b shows distinct steps in the frequency shift resulting from consecutive attachment of 250 nm gold particles (BBI Solutions, EMGC250), using cantilevers etched back to a length of 135 µm, with a thickness of 3.5 µm. This results in f_0=211.65 kHz and Q=150 in liquid. Including the tip mass, m_c is 29.7 ng and mass responsivity is -15mHz/fg. We find an average mass of 168±12 fg which agrees will with the expected value 175±68 fg based on TEM characterization of the particles. (See red histogram in Figure 5d). We confirm their real size using TEM imaging (JEOL, 2100-F). Figure 5c) shows a high-angle annular dark field image used to estimate the volume from the projected areas by assuming a spherical form factor. Only considering the particles with no occlusions we find an average

estimated mass of 174.6±68.3 fg. The large deviation as shown in figure 5d) is partly due to the different geometries deviating from perfect spheres. These data derive from cantilevers, which were not optimized for detecting exceedingly small masses but with the first flexural eigenmode and an amplitude Ac of 100 nm it results in a smallest detectable mass of 80 attogram/•Hz (See Eq. 1). Building the encasement around stiffer levers with shorter geometries has the potential to extend the frontier of biosensing in liquids down to the zeptogram range.

CONCLUSIONS

We have described successful fabrication of encasements around mechanical resonators the encasement traps an air bubble and thereby greatly reduces viscous damping. Improvements in performance by more than one order of magnitude for force sensing and nearly two orders of magnitude for mass sensing show that encased cantilevers revolutionize cantilever based sensing in liquids. Finite elements modeling and analytical expressions of hydrodynamic damping have been used to establish design rules for low squeeze film damping. The superior performance of encased cantilevers has been demonstrated imaging supported lipid bilayers and measuring the mass of gold nanoparticles.

ACKNOWLEDGEMENTS

The authors specifically thank E. Wong for fast and high-quality technical support, Virgina Altoe for her support in TEM imaging. We would like to thank Dr. Deirdre Olynick and Dr. Stefano Cabrini from the Nanofabrication Facility for fruitful discussions and their support in clean room processing. Work at Molecular Foundry was supported by the Office of Science, Office of Basic Energy Sciences, of the US Department of Energy under contract No. DE-AC02-05CH11231.

REFERENCES

[1] G. Binnig, C. F. Quate, and C. Gerber, “Atomic Force Microscope,” *Physical Review Letters*, vol. 56, no. 9, pp. 930+, 1986.

[2] Y. Martin and H. Wickramasinghe, “Magnetic imaging by "force microscopy‘’with 1000 Å resolution,” *Appl. Phys. Lett*, vol. 50, no. 20, pp. 1–3, 1987.

[3] W. J. Cho, A. Jeremic, and B. P. Jena, “Size of Supramolecular SNARE Complex: Membrane-Directed Self-Assembly,” *J. Am. Chem. Soc.*, vol. 127, no. 29, pp. 10156–10157, 2005/07/01 2005.

[4] A. Noy, D. V. Vezenov, and C. M. Lieber, “Chemical force microscopy,” *Annual Review of Materials Science*, vol. 27, no. 1, pp. 381–421, 1997.

[5] D. Ziegler and A. Stemmer, “Force gradient sensitive detection in lift-mode Kelvin probe force microscopy,” *Nanotechnology*, vol. 22, p. 075501, Jan. 2011.

[6] D. A. Walters, J. P. Cleveland, N. H. Thomson, P. K. Hansma, M. A. Wendman, G. Gurley, and V. Elings, “Short cantilevers for atomic force microscopy,” *Review of Scientific Instruments*, vol. 67, no. 10, pp. 3583–3590, 1996.

[7] P. Hansma, V. Elings, O. Marti, and C. Bracker, “Scanning tunneling microscopy and atomic force microscopy: application to biology and technology,” *Science*, vol. 242, no. 4876, pp. 209–216, Oct. 1988.

[8] H. G. Hansma and J. H. Hoh, “Biomolecular Imaging with the Atomic Force Microscope,” *Annual Review of Biophysics and Biomolecular Structure*, vol. 23, no. 1, pp. 115–140, 1994.

[9] J. Fritz, “Cantilever biosensors,” *Analyst*, vol. 133, no. 7, p. 855, Jan. 2013.

[10] J. L. Arlett, E. B. Myers, and M. L. Roukes, “Comparative advantages of mechanical biosensors,” *Nature Nanotechnology*, vol. 6, no. 4, pp. 203–215, Mar. 2011.

[11] A. Boisen, S. Dohn, S. S. Keller, S. Schmid, and M. Tenje, “Cantilever-like micromechanical sensors,” *Rep. Prog. Phys.*, vol. 74, no. 3, p. 036101, 2011

[12] H. Butt and M. Jaschke, “Calculation of thermal noise in atomic force microscopy,” *Nanotechnology*, vol. 6, no. 1, pp. 1–7, 1995.

[13] J. Sader, “Frequency response of cantilever beams immersed in viscous fluids with applications to the atomic force microscope,” *Journal of Applied Physics*, 1998.

[14] B. Sanii and P. D. Ashby, “High Sensitivity Deflection Detection of Nanowires,” *Physical Review Letters*, vol. 104, no. 14, Apr. 2010.

[15] T. E. Schaeffer, M. Viani, D. A. Walters, B. Drake, E. K. Runge, J. P. Cleveland, M. A. Wendman, and P. K. Hansma, “An atomic force microscope for small cantilevers,” *Proc. SPIE*, vol. 3009, p. 48, 1997.

[16] S. Torbrügge, O. Schaff, and J. Rychen, “Application of the KolibriSensor to combined atomic-resolution scanning tunneling microscopy and noncontact atomic-force microscopy imaging,” *Journal of Vacuum Science \& Technology B: Microelectronics and Nanometer Structures*, vol. 28, p. C4E12, 2010.

[17] T. van Zanten, M. Lopez-Bosque, and M. Garcia-Parajo, “Imaging Individual Proteins and Nanodomains on Intact Cell Membranes with a Probe-Based Optical Antenna,” *Small*, vol. 6, no. 2, pp. 270–275, 2010.

[18] J. M. LeDue, M. Lopez-Ayon, S. A. Burke, Y. Miyahara, and P. Gruetter, “High Q optical fiber tips for NC-AFM in liquid,” *Nanotechnology*, vol. 20, no. 26, p. 264018, Jun. 2009.

[19] M. Bao and H. Yang, “Squeeze film air damping in MEMS,” *Sensors and Actuators A: Physical*, vol. 136, no. 1, pp. 3–27, May 2007.

[20] T. Veijola, “Compact models for squeezed-film dampers with inertial and rarefied gas effects,” *J. Micromech. Microeng.*, vol. 14, p. 1109, 2004.

[21] C. R. Doering, “The 3D Navier-Stokes Problem,” *Annu. Rev. Fluid Mech.*, vol. 41, no. 1, pp. 109–128, Jan. 2009.

[22] C. P. Green and J. E. Sader, “Frequency response of cantilever beams immersed in viscous fluids near a solid surface with applications to the atomic force microscope,” *Journal of Applied Physics*, 2005.

[23] T. Naik, E. K. Longmire, and S. C. Mantell, “Dynamic response of a cantilever in liquid near a solid wall,” *Sensors and Actuators A: Physical*, vol. 102, no. 3, pp. 240–254, Dec. 2002.

[24] J. E. Sader, I. Larson, P. Mulvaney, and L. R. White, “Method for the calibration of atomic force microscope cantilevers,” *Review of Scientific Instruments*, vol. 66, no. 7, pp. 3789–3798, 1995.

[25] A. Sanpaulo, “High-Resolution Imaging of Antibodies by Tapping-Mode Atomic Force Microscopy: Attractive and Repulsive Tip-Sample Interaction Regimes,” *Biophysical Journal*, vol. 78, no. 3, pp. 1599–1605, Mar. 2000.

[26] D. Ebeling and H. Holscher, “Analysis of the constant-excitation mode in frequency-modulation atomic force microscopy with active Q-Control applied in ambient conditions and liquids,” *Journal of Applied Physics*, vol. 102, no. 11, p. 114310, 2007.

[27] J. Fritz, M. Baller, H. P. Lang, H. Rothuizen, P. Vettiger, E. Meyer, H. J. Guntherodt, C. Gerber, and J. K. Gimzewski, “Translating Biomolecular Recognition into Nanomechanics,” *Science*, vol. 288, no. 5464, pp. 316–318, Apr. 2000.

[28] A. Boisen, “Nanoelectromechanical systems: Mass spec goes nanomechanical,” *Nature Nanotechnology*, vol. 4, no. 7, pp. 404–405, Jul. 2009.

[29] S. Dohn, S. Schmid, F. Amiot, and A. Boisen, “Position and mass determination of multiple particles using cantilever based mass sensors,” *Appl. Phys. Lett*, vol. 97, no. 4, p. 044103, 2010.

[30] U. Rabe, J. Turner, and W. Arnold, “Analysis of the high-frequency response of atomic force microscope cantilevers,” *Appl Phys A*, vol. 66, no. 7, pp. S277–S282, Mar. 1998.

CONTACT

*P.D. Ashby, Tel: +1-510-486-7081; pdashby@lbl.gov